PLANETARY ROTATION AND STABILITY OF SATELLITE ORBITS

V. MIOC
Astronomical Institute of the Romanian Academy
Str. Cuţitul de Argint 5, RO-752121 Bucharest, Romania
e-mail: vmioc@aira.astro.ro

ABSTRACT. The planetary rotation acts on the satellite dynamics mainly via the zonal harmonics of the gravitational potential. We study the equatorial satellite orbits in a planetary fieldcharacterized by zonal harmonics up to the fifth order.

To depict the phase-space structure, we resort to McGehee-type coordinates, as well as to foliations by the energy constant and angular momentum constant. Various stability regions are found for each case.

The problem presents interesting features, as for instance: cases when all traiectories (except a separatrix) are stable; existence of stable motion for nonnegative energy levels; positive Lebesgue measure for initial data leading to quasiperiodic and noncircular periodic orbits; important role of the angular momentum.

1. INTRODUCTION

The planetary rotation influences the dynamics of a satellite primarily via the zonal harmonics of the gravitational potential (but through other effects, too). In this paper we study such an influence by tackling the equatorial motion of a satellite in the field of a planet featured by the potential

$$U = \sum_{n=1}^{6} a_n / r^n,$$

where r is the reciprocal distance, whereas a_n are real parameters. We consider $a_1 > 0$, $a_2 = 0$, $a_3 < 0$, as in the general planetary case in the solar system. Also, to obtain the most general situations, we considered the whole sign interplay among a_4, a_5, and a_6.

We work in collision-blow-up coordinates introduced by McGehee (1974). To identify the stability zones, we use the reduced 2D phase space, depicting all possible phase curves for negative, positive, and zero energy, for the collisional ($a_6 > 0$) and noncollisional ($a_6 < 0$) cases, and resorting to a foliation by the angular momentum. We find surprising stability regions for negative-energy levels (Figures 1a, 1d below), and even for nonnegative-energy levels. The stable orbits are either circular (relative equilibria) or noncircular (periodic and quasiperiodic). The initial data that lead to the latter ones have positive Lebesgue measure.

2. BASIC EQUATIONS

The two-body problem associated to our field can be reduced to a central-force problem.

The planar motion of the satellite with respect to the planet is described by the Hamiltonian $H(\mathbf{q},\mathbf{p}) = |\mathbf{p}|^2/2 - \sum_{n=1}^{6} a_n/|\mathbf{q}|^n$, where $\mathbf{q} = (q_1, q_2) \in \mathbf{R}^2 \setminus \{(0,0)\}$, $\mathbf{p} = (p_1, p_2) \in \mathbf{R}^2$ are the configuration vector and the momentum vector of the satellite, respectively. It is clear that the problem admits the first integrals of angular momentum ($q_1p_2 - q_2p_1 = L = \text{constant}$) and of energy ($H(\mathbf{q},\mathbf{p}) = h/2 = \text{constant}$).

To remove the isolated singularity at the origin $\mathbf{q} = (0,0)$, which corresponds to a collision (Mioc and Stavinschi 2001, 2002), we apply the following sequence of McGehee-type transformations (McGehee 1974):

$$\begin{aligned} r &= |\mathbf{q}|, \qquad \theta = \arctan(q_2/q_1), \\ \xi &= \dot{r} = (q_1p_1 + q_2p_2)/|\mathbf{q}|, \qquad \eta = r\dot{\theta} = (q_1p_2 - q_2p_1)/|\mathbf{q}|, \end{aligned} \tag{1}$$

which introduce standard polar coordinates,

$$x = r^3\xi, \qquad y = r^3\eta, \tag{2}$$

which scale down the velocity components, and a Sundman-type rescaling of time $d\tau = r^{-\alpha}dt$, $\alpha \in \mathbf{N}$. (This last transformation does not interest us in what follows.) In this way we obtain regular equations of motion. Under the transformations (1)−(2), the angular momentum integral and the energy integral become respectively

$$y = Lr^2, \tag{3}$$

$$x^2 + y^2 = hr^6 + 2\sum_{n=1}^{6} a_n r^{6-n}, \tag{4}$$

whereas the singularity at $r = 0$ was replaced by the collision manifold $M_0 = \{(r,\theta,x,y) \mid r = 0, \theta \in S^1, x^2 + y^2 = 2a_6\}$ pasted on the phase space.

The regularized equations of motion do not contain θ explicitly, so we can factorize the flow by S^1. Next, we eliminate y between (3) and (4). In this way the phase-space dimension was reduced from 4 to 2. The energy integral in the (r,x)-plane will read

$$x^2 = f(r) = hr^6 + 2a_1r^5 - L^2r^4 + 2a_3r^3 + 2a_4r^2 + 2a_5r + 2a_6,$$

where we took into account the fact that $a_2 = 0$. Remark that, in this plane, M_0 reduces to the points $\mathrm{M}(0, \sqrt{2a_6})$ and $\mathrm{N}(0, -\sqrt{2a_6})$.

We shall describe the phase-space structure for negative, zero, and positive energy levels, analyzing the behaviour of the function $x = \pm\sqrt{f(r)}$. Since $x^2 \geq 0$, we shall consider only the positive roots of the polynomial in the right-hand side of above energy integral. We also shall consider, for the same purpose, the positive roots of the polynomial $\tilde{f}(r) = df(r)/dr = 6hr^5 + 10a_1r^4 - 4L^2r^3 + 6a_3r^2 + 4a_4r + 2a_5$. To deal with the most general case, we suppose that $\tilde{f}(r)$ has four changes of sign (the maximum possible) for $h < 0$. This entails a maximum of five positive roots (according to Descartes' rule) for collisional phase-space ($a_6 > 0$) and four positive roots for noncollisional phase-space ($a_6 < 0$). For $h \geq 0$, we suppose that $\tilde{f}(r)$ has three changes of sign (the maximum possible, which entails a maximum of four/three positive roots for collisional/noncollisional phase-space.

3. PHASE-SPACE STRUCTURE

The phase-space structure for $h < 0$ is plotted in Figure 1. In the collisional case ($a_6 > 0$), there exists a critical energy level $h_c^- < 0$ that creates, along with the interplay of the field parameters, three different portraits: Figures 1a, 1b, 1c for $h < h_c^-$, $h = h_c^-$, and $0 > h > h_c^-$,

respectively. The foliation performed by making $|L|$ increase points out a great variety of phase orbits, as well as bifurcations (corresponding to critical values of L) concretized by relative equilibria: two centres S (stable circular orbits) and two saddles U (unstable circular orbits).

The case illustrated in Figure 1a is the most interesting. There are two kinds of quasiperiodic and periodic orbits. The ones bounded by the loop generated by U_1 and the double loop generated by U_2 (1) have significant osculating eccentricities. Those situated inside the double loop are centered on either S_1 (2) or S_2 (3) and have smaller osculating eccentricities. Such trajectories are recovered in Figures 1b (1', 2') and 1c (1", 2"). All these orbits are stable.

In the noncollisional case ($a_6 < 0$), there also exists a critical energy level, but all situations lead to the phase portrait plotted in Figure 1d. Except the separatrix formed by the double loop associated to the saddle $\bar{U}$ (which creates zones wholly similar to those in Figure 1a), all other orbits are stable.

The phase-space structure for $h > 0$ is plotted in Figure 2. There also exist critical values of the energy level, which create three different phase portraits for $a_6 > 0$, or only one portrait for $a_6 < 0$. The stability zones lie inside the homoclinic loop associated to the saddles U_2 (Figure 2a), U_2" (Figure 2c), $\bar{U}$ (Figure 2d), or inside the heteroclinic loop created by the saddles U_1' and U_2' (Figure 2b). These stable orbits are quasiperiodic or periodic, and are centered on the equilibria S, S', S", $\bar{S}$ (all stable circular orbits).

The case $h = 0$ leads to exactly the same phase portraits as in Figure 2, but now the different pictures are generated only by the interplay of the field parameters.

4. CONCLUDING REMARKS

To search for stability regions in our problem, we depicted the phase portraits for the whole interplay among field parameters, energy level, and angular momentum. The most important features of the model (some of them surprising) are:

4.1. For $h < 0$, there exist cases (Figures 1a, 1d) in which a double loop associated to a saddle creates three zones of stable quasiperiodic and periodic orbits. Moreover, in Figure 1d all trajectories (but the separatrix) are stable.

4.2. There exist quasiperiodic and periodic orbits even for nonnegative energy levels.

4.3. The sets of quasiperiodic and noncircular periodic orbits have positive Lebesgue measure. Indeed, choosing initial data on such an orbit, and considering the foliations performed, in a neighbourhood of this point there exists an open set of initial data that lead to the same kind of orbit.

4.4. The role of the angular momentum is of the same importance as that of the energy. It creates bifurcations without regard to the energy level.

4.5. Our results were obtained for the maximum number of changes of sign of $\tilde{f}(r)$. Simpler mathematical situations entail simpler phase portraits. For instance, in the Earth's case, the phase-space structure is similar to that of Fock's problem (Mioc and Pérez-Chavela 2003): only one type of stable orbits for $h < 0$, and no stable orbit for $h \geq 0$.

4.6. Our results can add something to the explanation of the observed structure of the planetary rings, especially as concerns the existence of gaps.

5. REFERENCES

McGehee, R.: 1974, *Invent. Math.* **27**, 191.
Mioc, V., Stavinschi, M.: 2001, *Phys. Lett. A* **279**, 223.
Mioc, V., Stavinschi, M.: 2002, *Phys. Scripta* **65**, 193.
Mioc, V., Pérez-Chavela, E.: 2003, *J. Math. Phys.* **44** (to appear).

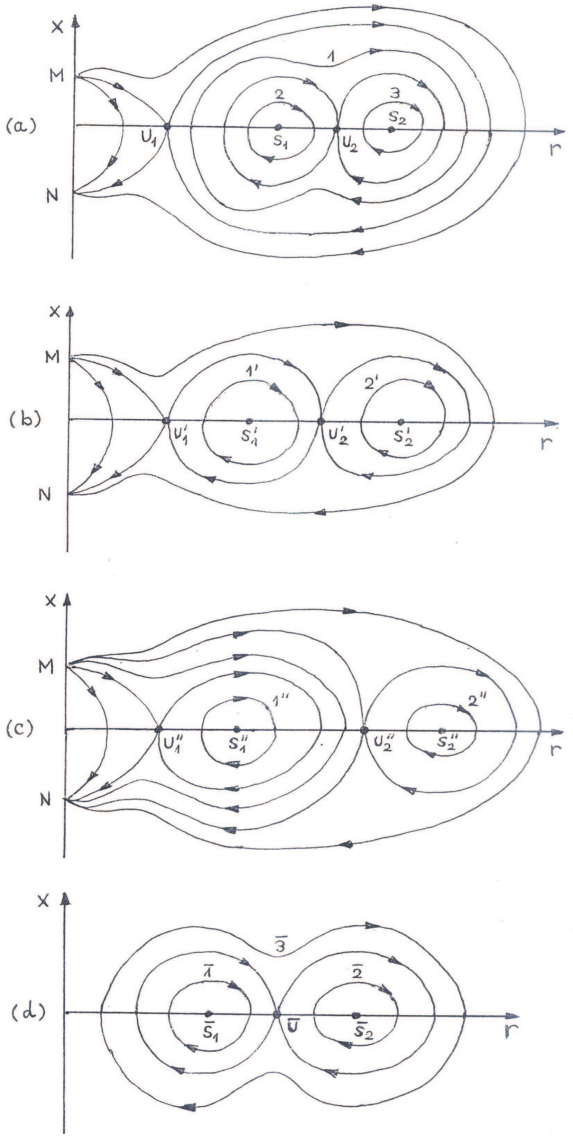

Figure 1: The phase portrait for $h < 0$, in the collisional case, for (a) $h < h_c^-$, (b) $h = h_c^-$, (c) $0 > h > h_c^-$, and in the noncollisional case (d).

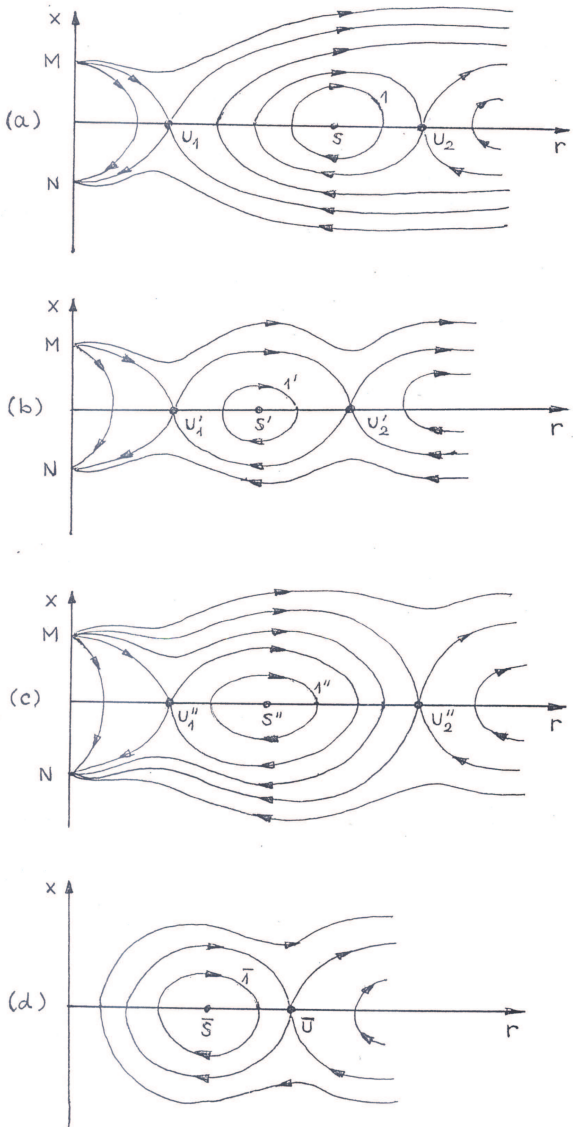

Figure 2: The phase portrait for $h \geq 0$, in the collisional case, for (a) $h < h_c^-$, (b) $h = h_c^-$, (c) $0 > h > h_c^-$, and in the noncollisional case (d).